NREL
NATIONAL RENEWABLE ENERGY LABORATORY

Examination of an Optical Transmittance Test for Photovoltaic Encapsulation Materials

Preprint

David C. Miller,[a] Jaione Bengoechea,[b] Jayesh G. Bokria,[c] Michael Köhl,[d] Nick E. Powell,[e] Michael E. Smith,[f] Michael D. White,[g] Helen Rose Wilson,[d] and John H. Wohlgemuth [a]

[a]*National Renewable Energy Laboratory*
[b]*Fundación CENER-CIEMAT*
[c]*Specialized Technology Resources, Inc.*
[d]*Fraunhofer-Institut für Solare Energiesysteme ISE*
[e]*Dow Corning Corp.*
[f]*Arkema Inc.*
[g]*The Dow Chemical Company*

Presented at SPIE Optics & Photonics 2013
San Diego, California
August 25–29, 2013

NREL is a national laboratory of the U.S. Department of Energy
Office of Energy Efficiency & Renewable Energy
Operated by the Alliance for Sustainable Energy, LLC

This report is available at no cost from the National Renewable Energy Laboratory (NREL) at www.nrel.gov/publications.

Conference Paper
NREL/CP-5200-60029
September 2013

Contract No. DE-AC36-08GO28308

This report is available at no cost from the National Renewable Energy Laboratory (NREL) at www.nrel.gov/publications.

Available electronically at http://www.osti.gov/bridge

Available for a processing fee to U.S. Department of Energy and its contractors, in paper, from:

U.S. Department of Energy
Office of Scientific and Technical Information
P.O. Box 62
Oak Ridge, TN 37831-0062
phone: 865.576.8401
fax: 865.576.5728
email: mailto:reports@adonis.osti.gov

Available for sale to the public, in paper, from:

U.S. Department of Commerce
National Technical Information Service
5285 Port Royal Road
Springfield, VA 22161
phone: 800.553.6847
fax: 703.605.6900
email: orders@ntis.fedworld.gov
online ordering: http://www.ntis.gov/help/ordermethods.aspx

Cover Photos: (left to right) photo by Pat Corkery, NREL 16416, photo from SunEdison, NREL 17423, photo by Pat Corkery, NREL 16560, photo by Dennis Schroeder, NREL 17613, photo by Dean Armstrong, NREL 17436, photo by Pat Corkery, NREL 17721.

Printed on paper containing at least 50% wastepaper, including 10% post consumer waste.

Examination of an Optical Transmittance Test for Photovoltaic Encapsulation Materials

David C. Miller,[a] Jaione Bengoechea,[b] Jayesh G. Bokria,[c] Michael Köhl,[d] Nick E. Powell,[e] Michael E. Smith,[f] Michael D. White,[g] Helen Rose Wilson,[d] and John H. Wohlgemuth[a]*

[a]National Renewable Energy Laboratory, 15013 Denver West Parkway, Golden, CO, USA 80401
[b]Fundación CENER-CIEMAT, C/Ciudad de la Innovación 7, Sarriguren, Spain 31621
[c]Specialized Technology Resources, Inc., 18 Craftsman Road, East Windsor, CT, USA 06088
[d]Fraunhofer-Institut für Solare Energiesysteme ISE, Heidenhofstr. 2, 79110 Freiburg, Germany
[e]Dow Corning Corp., 2200 W. Salzburg Rd, Midland MI, USA 48686
[f]Arkema Inc., 900 First Avenue, King of Prussia, PA, USA 19406
[g]The Dow Chemical Company, 1605 Joseph Drive, 200 Larkin, Midland, MI, USA 48667

ABSTRACT

The optical transmittance of encapsulation materials is a key characteristic for their use in photovoltaic (PV) modules. Changes in transmittance with time in the field affect module performance, which may impact product warranties. Transmittance is important in product development, module manufacturing, and field power production (both immediate and long-term). Therefore, an international standard (IEC 62788-1-4) has recently been proposed by the Encapsulation Task-Group within the Working Group 2 (WG2) of the International Electrotechnical Commission (IEC) Technical Committee 82 (TC82) for the quantification of the optical performance of PV encapsulation materials. Existing standards, such as ASTM E903, are general and more appropriately applied to concentrated solar power than to PV. Starting from the optical transmittance measurement, the solar-weighted transmittance of photon irradiance, yellowness index (which may be used in aging studies to assess durability), and ultraviolet (UV) cut-off wavelength may all be determined using the proposed standard. The details of the proposed test are described. The results of a round-robin experiment (for five materials) conducted at seven laboratories to validate the test procedure using representative materials are also presented. For example, the Encapsulation Group actively explored the measurement requirements (wavelength range and resolution), the requirements for the spectrophotometer (including the integrating sphere and instrument accessories, such as a depolarizer), specimen requirements (choice of glass-superstrate and -substrate), and data analysis (relative to the light that may be used in the PV application). The round-robin experiment identified both intra- and inter-laboratory instrument precision and bias for five encapsulation materials (encompassing a range of transmittance and haze-formation characteristics).

Keywords: material characteristics, quality assurance, accelerated stress testing, reliability, polymer

1. INTRODUCTION

Optical transmittance is a key performance characteristic for photovoltaic (PV) encapsulation materials. The discoloration of encapsulation (and corresponding reduction in transmittance) has also been identified as a key contributor to the long-term performance degradation of fielded PV modules [1]. Existing standards—including ISO 13468 [2], ASTM E903 [3], ASTM E1175 [4], and ASTM E424 [5]—do not examine the relevant parameter (the photon irradiance, $E_{p\lambda}$, $\{m^{-2}\cdot s^{-1}\cdot m^{-1}\}$) or make use of analysis that may be used to further assess PV encapsulation, including yellowness index (*YI,* {unitless}) and UV cut-off wavelength (λ_{cUV}, {m}). The Encapsulation Committee within the International Electrotechnical Commission (IEC) Technical Committee 82 (TC82) on PV Working Group 2 (WG2) on PV modules has created a standard material-level test to assess the expected optical performance of encapsulation at its interface with the PV cell. The protocol, colloquially known as the "transmittance standard," describes the measurement of optical transmittance and subsequent analysis of $E_{p\lambda}$, *YI*, and λ_{cUV}. The purpose of the standard is to aid material manufacturers and module manufacturers in performing material acceptance, material or process development, design analysis, and failure analysis. No "pass" or "fail" criteria are assigned for the proposed test procedure; rather, it is intended to be used for datasheet reporting, quality control, and durability assessment.

*David.Miller@nrel.gov; phone: +1-303-384-7855; fax: +1-303-384-6490; www.nrel.gov/pv/performance_reliability/

The standard specifies to measure the transmittance (τ, {unitless}) from 300 to 2500 nm in a 1-nm increment using a double-beam spectrophotometer, as in [2],[3],[4],[5]. The standard uses the photon irradiance (Equation 1), which considers number of photons rather than the raw incident energy. This is done because one photon can produce at most one electron-hole pair in a typical PV cell. The solar-weighted transmittance of photon irradiance (Equation 2) considers the measured τ relative to the $E_{p\lambda}$ of the solar source, defined in Ref. [6]. Following Ref. [7], new parameters in the equations include: λ, the wavelength {m}; E_λ, the spectral irradiance {W•m^{-2}•m^{-1}}; h, Planck's constant {6.626·10^{-34} W·s^2}; c, the speed of light in a vacuum {2.998·10^8 m·s^{-1}}; and τ_w, the weighted transmittance {unitless}.

$$E_{p\lambda}[\lambda] = \frac{\lambda}{hc} E_\lambda[\lambda] \tag{1}$$

$$\tau_w = \frac{\int \tau[\lambda] E_{p\lambda}[\lambda] d\lambda}{\int E_{p\lambda}[\lambda] d\lambda} \tag{2}$$

The "solar-weighted" transmittance (τ_{sw},{unitless}), obtained using Equation 2, is defined for $300 \le \lambda \le 2500$ nm. τ_{sw} is intended to be used as a figure of merit that may be applied to all PV, regardless of the cell technology. The "representative solar-weighted" transmittance (τ_{rsw},{unitless}) is also determined from Equation 2, but is defined for $300 \le \lambda \le 1250$ nm. τ_{rsw} considers the typical maximum operating wavelength range for contemporary flat-panel PV devices. Figure 1 shows the external quantum efficiency (EQE) profiles for champion cell technologies, documented in the publication series of Ref. [8]. The figure identifies spectral performance for cell technologies including InGaP/GaAs/InGaAs multijunction (3J), gallium arsenide single-junction (GaAs), monocrystalline silicon (m-Si), copper-indium-gallium-selenide (CIGS), polycrystalline silicon (p-Si), cadmium-telluride (CdTe), and copper-zinc-tin-sulfur-selenide (CZTSS), relative to the AM1.5 solar spectrum [6]. The λ_{cUV} and infrared (IR) regions are examined to the left and right of Figure 1, respectively. The insets of the figure confirm that the spectral bandwidth for the cell technologies occurs within $300 \le \lambda \le 1250$ nm (except for 3J, which extends up to 1800 nm).

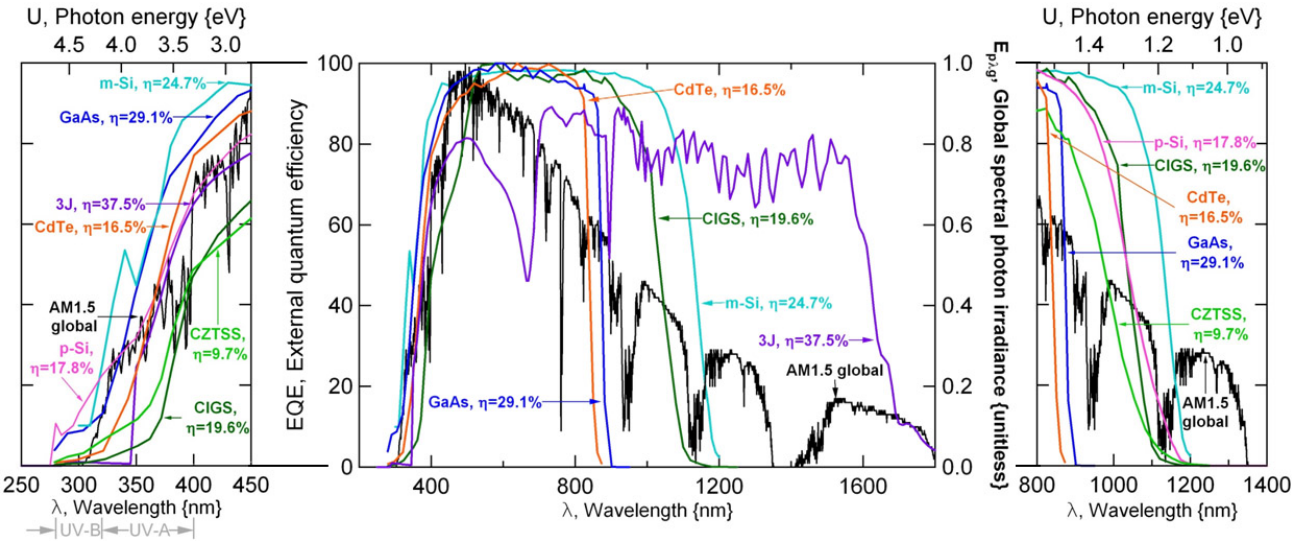

Figure 1: Representative EQE profiles for popular PV device technologies shown relative to the global terrestrial solar spectrum (AM1.5 in IEC 60904-3).

YI is determined in the standard for a D65 illuminant (mid-day outdoor sun, as in Ref. [9]) for a human observer (CIE 1964 XYZ color space with 10° field of view, as in Ref. [10]). The illuminant and observer data are tabulated in the ISO standards for a 1-nm increment, rather than the 5-nm tabulated data in the comparable ASTM standards, *i.e.*, [11],[12]. *YI* is a metric of how much absorption occurs in the blue wavelengths and is weighted by the D65 spectrum and the efficacy of the cone receptors of the human eye. A yellowness of 0.00, considered neutral, indicates no optical

absorption between 360 and 830 nm. A positive value indicates yellowing from absorption in the blue region of the spectrum, and a negative value indicates a shift toward blue due to absorption in the red region of the spectrum. The calculation of *YI* may be performed using numerical integration, which provides the three tri-stimulus values (corresponding to the three cone types), a normalizing factor, and two other coefficients [10],[12]. The *YI* of polymers tends to increase with age with the development of chromophore species, which would be perceived as yellow or brown (in worst cases) by a human observer.

Like YI, λ_{cUV} may be used to assess the weathering of polymers. The critical consideration for the standard is whether a low, medium, or high threshold (*e.g.*, τ = 10, 50, or 90%) is preferred for λ_{cUV}. The steps in the protocol recommended by Ametek, Inc., include: 1) determine the value of the maximum measured τ; 2) determine the λ at the τ = 72% of the maximum τ; 3) determine the λ at the τ = 50% of the maximum τ; 4) linearly extrapolate λ_{cUV} (defined at the τ = 5%) from τ = 72% and τ = 50%. The Ametek method is advocated because rapid transitions in optical transmittance were found to be difficult to replicate between different instruments, *e.g.*, limited by the finite rates of scanning and detection. The Ametek method to determine λ_{cUV} was therefore established experimentally, based on the measured reproducibility within and between separate laboratories.

Several criteria for the determination of λ_{cUV} were identified early in the creation of the test standard, including: the absolute τ of 10%; the Ametek method (described above for the relative τ, projected to 5%); the absolute τ of 1%; and the absolute τ of 50%. The criterion of 10% (which corresponds to an optical absorbance of 1) was the most widely cited in the literature. It comes from the biological and nanosciences, where it is often applied to liquid specimens measured in a 1-cm cuvette. The criterion of 1% is used in some of the physical sciences, where it is considered as the threshold for biologically affecting solar radiation. The criterion of 50% is common in applications such as photographic filters.

The standard specifies to use silica/polymer (for datasheet reporting) or silica/polymer/silica specimens (for durability studies). The silica/polymer geometry simulates the application (up to the interface with the PV cell) when the polymer surface faces the entrance of the integrating sphere. The silica/polymer/silica geometry is anticipated to contain both aerobic (at the edges) and anaerobic (at the interior) regions during aging in air, for specimens ~50-mm x~50-mm or greater in size. Users may wish to verify this assumption. The glass is specified to be 3±1mm thick (including the popular 3.2-mm "double-strength" glass found in flat-panel PV). The glass used for datasheet reporting cannot have texture, coatings, or antireflective (AR) layer(s). Any glass may be used in tests performed for other purposes.

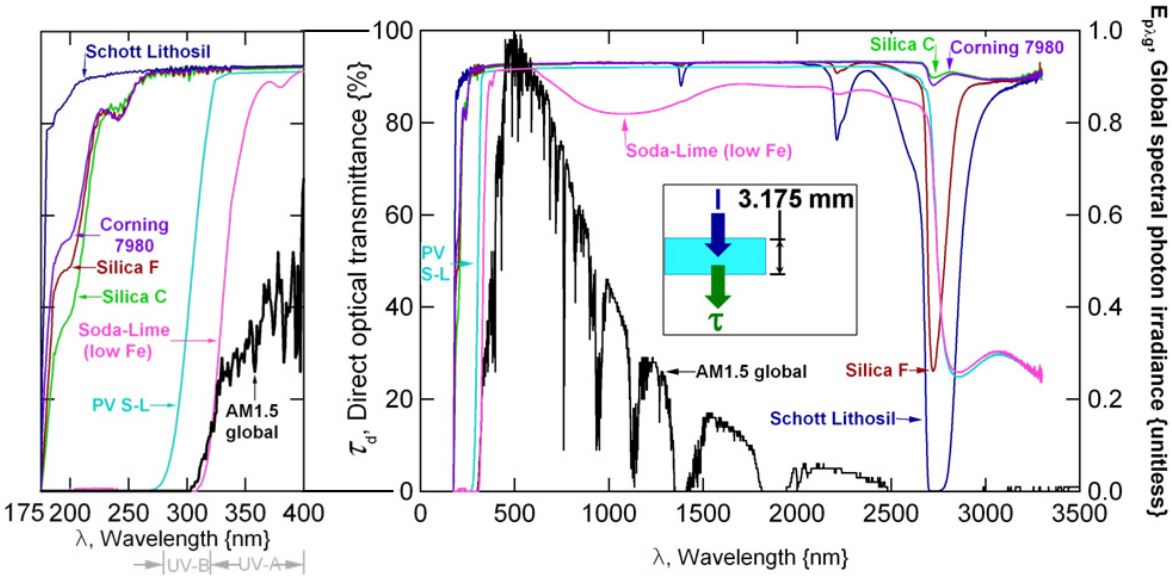

Figure 2: Measured τ for two silica glass specimens relative to commercial "quartz" and soda-lime glass products, as well as the global terrestrial solar spectrum (AM1.5 in IEC 60904-3).

The measured τ for two appropriate silica glass specimens is shown in Figure 2, relative to commercial "quartz" and soda-lime glass products. Figure 2 shows examples of soda-lime glass including both low-iron ("low-Fe") and PV-specific glass ("PV S-L"). The examples of "quartz" glass, 7980 (Corning Inc.) and Lithosil (Schott AG), are included along with the AM1.5 solar spectrum [6]. The direct transmittance (τ_d, obtained without an integrating sphere, unlike in the standard) is shown in Figure 2, because of the greater wavelength range that can be obtained ($175 \le \lambda \le 3300$ nm) for material verification. The measured τ for the specimens of different thickness were compensated to the thickness (z, {m}) of 3.2 mm, as described in Ref. [13] and indicated in Figure 2.The inset left of the figure shows the transmittance at short wavelengths, including the UV, where the "UV-A" and "UV-B" bands are labeled. The same specimens shown in Figure 2 are summarized in Table 1. The values for the specimen thickness (measured using a micrometer), τ_{sw}, τ_{rsw}, *YI*, and λ_{cUV} (determined for 10% of the absolute measured τ) are given in the table. The data averages (x) for the silica specimens are also provided in Table 1. As in Figure 2, the data in Table 1 have been analyzed to compensate the results to $z = 3.2$ mm. In general, the silica specimens have a τ_{sw} of 93%, τ_{rsw} of 93%, *YI* of 0.2, and λ_{cUV} of 179 nm. λ_{cUV} is listed; however, the wavelength limit below which it can be accurately measured in an ambient atmosphere containing moisture was not examined further. The seven silica specimens all demonstrate optical transmittance intermediate to the Lithosil (considered an "optical"-grade quartz) and 7980 (a "fused silica"). In particular, silica C and 7980 exhibit a minor–OH absorption band at 2750 nm, suggesting minimal residual water content. The soda-lime glasses have a reduced τ relative to the silica specimens, which are purer in content. In Figure 2, the low-Fe soda-lime specimen uniquely demonstrates the Fe absorption band about 1075 nm. The PV-specific soda-lime glass in Figure 2 transmits UV-B radiation, whereas the low-Fe soda-lime specimen transmits UV-A only. The characteristics of silica include: UV transparency—it will minimally affect the transmittance measurements of intermediate polymer layers (compare λ_{cUV} in Table 1 to λ_{cUV} in Table 6); immunity to corrosion in hot-damp aging environments; an outer surface may be readily cleaned with solvents (*e.g.*, toluene, isopropyl alcohol, water) to remove contamination or residual polymer.

Table 1: Summary of the glass specimens ("silica A" – "silica G") used in the round-robin experiment, described below.

SPECIMEN	z, SPECIMEN THICKNESS {mm}	τ_{sw} {%}	τ_{rsw} {%}	*YI* {unitless}	λ_{cUV} {nm}
A	3.2	92.86	92.78	0.17	178
B	3.2	92.56	92.84	0.20	177
C	2.9	92.79	92.67	0.26	180
D	1.6	92.78	92.81	0.22	181
E	1.5	92.74	92.75	0.16	181
F	3.1	92.85	92.82	0.18	178
G	3.2	92.79	92.76	0.17	178
x, Avg	**N/A**	**92.77**	**92.77**	**0.19**	**179**
S-L (Low Fe)	5.6	86.53	86.46	-0.06	320
PV S-L	3.2	91.87	91.80	0.29	289
7980	5.3	92.88	92.82	0.12	176
Lithosil	5.9	92.48	92.77	0.14	176

Many polymeric materials are birefringent, having a refractive index (n) that depends on the polarization and propagation direction of light. These materials may generate measurement error in some spectrophotometers because they modify the polarization state of transmitted light passing through the instrument optics and onto the detectors, even after measurement baselines have been performed. To mitigate this effect, a depolarizer, included in the baseline, can be placed before the sample. Figure 3 shows the τ for a glass/polymer/glass specimen, measured on the same spectrophotometer, with and without a depolarizer present. A section view of the measurement and specimen geometry is shown in the inset of Figure 3. The individual measurements were obtained well after the instrument had been activated, so that the lamp emission and instrument detection had stabilized to their steady-state operation. A

discontinuity occurs at 900 nm in the measurement where no depolarizer is present. Discontinuities, such as that shown in Figure 3, may result from changes in the optics (*e.g.*, the detector and grating changeovers) or source used within the spectrophotometer. As shown in Figure 3, the effect of birefringence is minimized when a depolarizer is used. A change in stress, which also affects the polarization state in a birefringent specimen, occurring over time (*e.g.*, with aging) would further misconstrue the transmittance measurement. The effects of residual moisture absorbed during aging, which can scatter and attenuate light in a τ measurement, are described in Ref. [14]. An optical image (obtained using cross-polarization photography) is shown in the inset of Figure 3. Cross-polarization photography may be used on materials like ethylene-co-vinyl acetate or polyolefin to identify polarization sensitivity or to qualitatively visualize stress within a specimen, based on color or brightness contrast within the image.

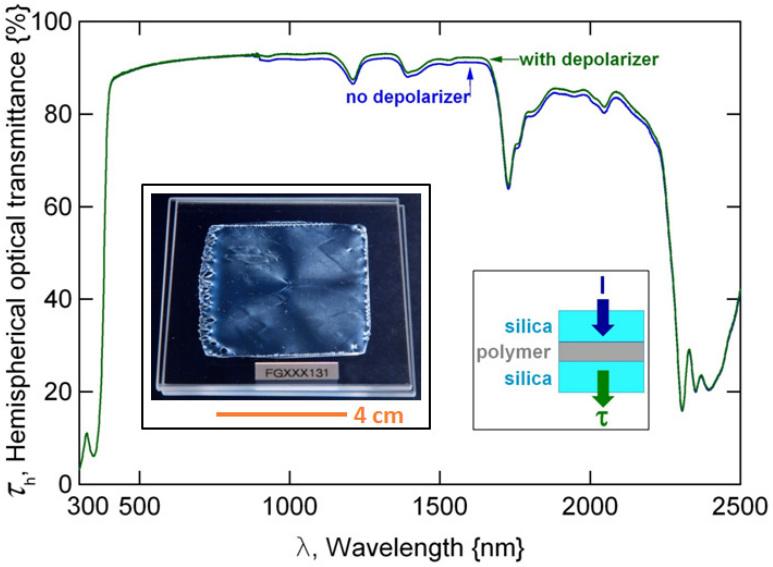

Figure 3: τ for a glas/polymer/glass specimen, measured on the same spectrophotometer, with and without a depolarizer present.

The goal of the described experiments was to support the development of a standardized test procedure that can be used to evaluate the optical transmittance of encapsulation products intended for use in PV modules. Discovery experiments were used to examine issues, including: the variability of representative silica glass specimens; the use of a single-beam or double-beam spectrophotometer instrument; and the variability of transmittance for specimens using the same encapsulation material, but constructed in different laboratories. A round-robin experiment was conducted to determine the intralaboratory repeatability and interlaboratory reproducibility for the test standard, as well as to develop the test procedure, *e.g.*, select the criteria for the UV cut-off wavelength.

2. EXPERIMENTAL

2.1 Details of the Round-Robin Experiment

A round-robin experiment (R-R) was conducted according to Ref. [15] (which describes the design and implementation) and Ref. [16] (which describes the analysis and interpretation of the results). Table 2 summarizes the spectrophotometer instruments used in the R-R. Characteristics listed in the table include the make and model of the instrument, inner diameter of the integrating sphere, beam size at the specimen (given to the nearest mm), incident angle (at the reflector port), presence/use of a depolarizing optic, ratio of the area of the open ports to that of the sphere walls (plus all the ports), material for the walls of the integrating sphere, and type of detectors. All of the instruments use a deuterium lamp as a UV light source and a halogen lamp for the visible and IR wavelengths. Although the maximum active range is listed in Table 2 for the detectors, the active range is typically reduced (*e.g.*, 200–2600) by the range of reflectance of the sphere material. Practically speaking, a nitrogen gas purge is required to improve the quality of optical measurements for $\lambda < 250$ nm. All of the instruments were double-beam spectrometers, except the single-beam CENER instrument. Use of a depolarizing optic may reduce the measurement range to ~275 nm, depending on its composition. Six different

instruments, with some replicates (two Lambda 950's and two Cary 5000's) were used. A photomultiplier tube (PMT) was used for UV-Vis detection, except at CENER, where CCD arrays were used.

Four types of material were examined in the R-R: ethylene-co-vinyl acetate (EVA), ionomer, poly(dimethylsiloxane) (PDMS), and thermoplastic polyolefin (TPO). For one of the materials, both a hazy and non-hazy formulation was used to specifically examine the results for a material prone to light-scattering. The material types will not be identified in the R-R results. The material types are omitted to prevent misinterpretation of the transmittance results (the rank of materials examined), which can depend highly on the specific formulation of the materials examined. Both glass/polymer and glass/polymer/glass specimen geometries (three replicates each) were examined for each material. Specimens were cleaned on their exposed glass surfaces with isopropyl alcohol prior to measurement, except for the PDMS specimens, which were first cleaned with toluene.

Table 2: Summary of the spectrophotometer instruments used in the round-robin experiment.

LABORATORY	INSTRUMENT MAKE	INSTRUMENT MODEL	DIAMETER, SPHERE {mm}	BEAM SIZE {mm x mm}	INCIDENT ANGLE {°}	DEPOLARIZER ?	RATIO: PORTS/ SPHERE{%}	SPHERE MATERIAL	TYPE OF DETECTORS (ACTIVE RANGE {nm})
Arkema	Perkin-Elmer	Lambda 950	150	10 x 16	8	CBD present, not used	12.8	Spectralon	PMT (175 – 860) PbS [cooled] (861 – 3300)
CENER	Instrument Systems GmbH	Custom	150	Ø 20	8	No	1.4	$BaSO_4$	CCD Arrays, Si (200-850) InGaAs (800-1650)
Dow Chemical	Perkin-Elmer	Lambda 950	60	12 x 15	O	CBD present, not used	12.8	Spectralon	PMT (175 – 860) PbS [cooled] (861 – 3300)
Dow-Corning	Agilent	Cary 5000	110	11 x 13	3.33	Yes	3	PTFE	PMT (175 – 800) PbS [cooled] (800 – 3300)
Fraunhofer	Perkin-Elmer	Lambda 900	220	10 x 16	8	CBD present, not used	1.9 (1.4)	Sintered PTFE	PMT (175 – 860) PbS [cooled] (861 – 3300)
NREL-1	Agilent	Cary 5000	150	4 x 12.5	7	CBD present, not used	4.9	PTFE	PMT (175 – 800) PbS [cooled] (800 – 3300)
NREL-2	Shimadzu	UV-3600	60	3 x 10	8	No	4.6	$BaSO_4$ (Barium Sulfate)	PMT (175-740) InGaAs (740-1650) PbS (1650-3300)
STR	Perkin-Elmer	Lambda 1050	150	8 x 16	8	No	2.5	Spectralon	PMTTube (175-860) InGaAs (861-3300)

2.2 Details of the Discovery Experiments

Several discovery experiments were conducted in conjunction with the R-R. First, the silica (procured separately from different sources by the participating laboratories) was all measured at NREL. The results, presented in Figure 2 and Table 1 quantify the characteristics of silica glass appropriate for the transmittance test. A single-beam spectrophotometer was used at one laboratory to examine typical instrument performance and identify possible issues relative to double-beam instruments. This second experiment used the same five specimen sets circulated in the R-R. The variability of specimen fabrication was also examined in addition to the R-R. Here, the laboratory participants were supplied uncured EVA sheet and instructed upon its intended processing by the material manufacturer. The laboratory participants also had to procure silica glass from their chosen vendor. The variability of specimens constructed from the same EVA was compared by measuring all the EVA specimens at NREL. Representative glass/polymer (g/p) and glass/polymer/glass (g/p/g) EVA specimen sets (all specimens within each set made at the same laboratory) were then chosen for the R-R. In the fourth experiment, the same single glass/EVA/glass specimen was measured in each laboratory ten times without replacement (the specimen was not moved between measurements) and ten times with replacement (the specimen was removed from and then replaced into the instrument before each measurement).

3. RESULTS AND DISCUSSION

The use of a single-beam (SB) spectrophotometer is examined in Figure 4, where representative data profiles (one of the three replicates, for both g/p and g/p/g specimens) are compared to those obtained using a double-beam (DB) instrument. The baseline for the SB measurements in Figure 4 was performed with no specimen present at the entrance port of the integrating sphere. The SB measurements were then performed with the specimen placed over the entrance port of the integrating sphere. A section view of the specimen geometry and uncompensated measurement is shown in the inset of Figure 4. The AM1.5 solar spectrum [6] is also shown in the figure for reference. A substantial (~1.3% difference in τ_W) occurs in Figure 4 between SB and DB measurements. An additional ~0.6% difference in τ_W occurs in Figure 4 between g/p/g and g/p specimens for both the SB and DB measurements. Separately, measurement noise (associated with the detector and grating used below ~900 nm is observed in Figure 4, particularly for the DB measurements.

There is a notable difference between the SB and DB measurements that is attributed to port effects. When a baseline is performed without a specimen in place and then a specimen is placed for measurement at the sample port, the specimen increases the reflectivity of the port and total light-trapping of the sphere. This increases the measured signal relative to the baseline, resulting in erroneously high transmittance measurements. To facilitate proper SB measurements, the baseline was first performed with a specimen on the reflectance port of the integrating sphere, but with the beam first striking the sphere wall (requiring a double-beam sphere or sphere designed for off-axis use) rather than the sample. Measurements were then performed with the specimens on entrance port of the integrating sphere, enabling automatic measurement correction of the port effects. Using that measurement procedure, the SB data could not be readily distinguished from DB data (outside of the measurement variability between laboratories, not shown). Regarding the difference between the g/p/g and g/p specimens, the τ_w was typically greater for the g/p/g specimens. Here, the difference is attributed to the index mismatch between the back surface of the specimen and air. The refractive index of most of the PV encapsulation materials examined is greater than that of silica glass [13]. The least reflectance loss (and corresponding greatest transmittance) is therefore expected for the g/p/g specimens, where *n* of the silica back surface is best matched to air. It should be noted that a very different index mismatch will occur in air (n = 1.0003) than at the polymer/cell interface, because the *n* of the cell is greater, *e.g.*, the *n* of a Si_3N_4 antireflective surface layer is ~ 2.0. Lastly, the greater noise observed in the UV-Vis data for all the materials is attributed to the limitations of the instrument technology (*e.g.*, detectors) as well as the UV scattering from airborne moisture.

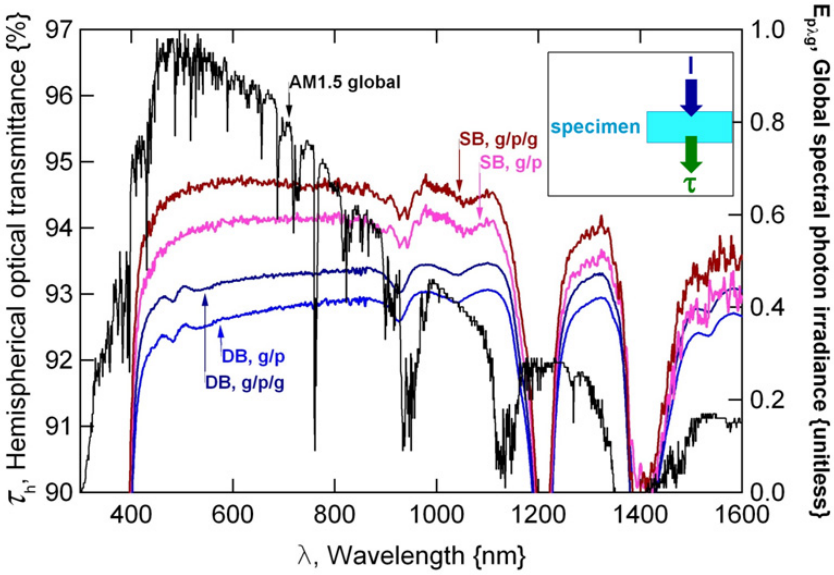

Figure 4: Comparison of single-beam (uncorrected) and double-beam instrument measurements (representative profiles) for glass/polymer and glass/polymer/glass specimens.

The measured transmittance for the hazy material (averaged for the three replicate specimens) is shown in Figure 5. All specimen data are from the glass/polymer/glass configuration, as indicated in the figure inset. The *haze* {unitless}, calculated as *haze* = $(\tau_h-\tau_d)\cdot\tau_h^{-1}$, is also shown where it may be applied in Figure 5. The *haze* was determined for the NREL-1 instrument. The AM1.5 solar spectrum [6] is also shown in Figure 5. An increase in *haze* is observed as the wavelength is decreased, identifying increased optical scattering at shorter wavelengths. The τ_h profiles for the other materials corresponded well, essentially overlapping between instruments. There are considerable differences, however, between the measurements for the hazy material in Figure 5. In the figure, the NREL-2 τ_h profile is notably less than the other τ_h profiles. The NREL-2 results were repeatable between measurement sessions.

The disparity between the measurements in Figure 5 is thought to be related to the different angles of acceptance for the different makes of spectrophotometer instruments, including the position of the detector with respect to the entrance port. For example, the Dow-Corning and NREL-1 data (both obtained using a Cary 5000) nearly overlap, as would be expected for the same make of instrument. *Haze* may result in polymers from spherulite size and concentration. Because the haze depends on the refractive index of the crystallite and amorphous regions within the polymer, scattering will vary

with wavelength. The effect becomes critical to transmittance measurements if the scattered light falls outside of the acceptance angle of the spectrophotometer. Unfortunately, the acceptance angle is typically not specified by the manufacturer. Furthermore, the reflectance spectrum of the interior sphere wall is neither easily determined nor constant with time. The results in Figure 5 are not attributed to the aging of the specimen, *e.g.*, no overt trend was observed over the course of the measurements and the NREL-2 measurements were performed first. The behavior in Figure 5 could be of concern in aging studies, however, if discolored/aged material were prone to haze formation. In such cases, the transmittance results would be instrument dependent.

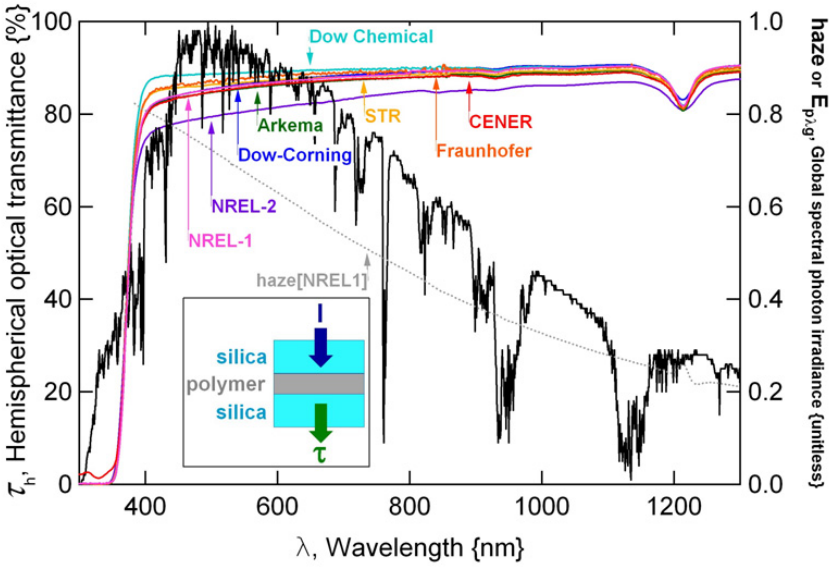

Figure 5: Measured transmittance for the haze-generating material. The *haze*, determined from the hemispherical transmittance (τ_h) and direct transmittance (τ_d, where no integrating sphere is present) for the "NREL-1" instrument, is also shown, relative to the global terrestrial solar spectrum (AM1.5 in IEC 60904-3).

The results of the measurements for the EVA specimens made at the different laboratories are summarized in Table 3. Data in the table include the characteristics of τ_{sw}, the τ_{rsw}, *YI*, and λ_{cUV} (10% absolute criterion) for the seven sample sets. The average (x), standard deviation (s_x, 1σ), repeatability (s_r, nominal), and reproducibility (s_R, nominal) are identified in Table 3 for each of the four characteristics. As defined in Ref. [16], repeatability addresses the question, "What is the average of the variance for the laboratories, *i.e.*, how tightly clustered are the data within each laboratory?" If each laboratory had a small variation, then s_r would be minimal, even if the variation between the different laboratories was substantial. As defined in Ref. [16], reproducibility considers the deviation of the laboratory averages from the average of the experiment as well as the repeatability, weighted by the number of samples. Reproducibility therefore quantifies, "How well do the data sets overlap, and how tightly clustered are the data within each laboratory (s_r)?" s_r and s_R in Table 3 apply to specimens made at different laboratories, rather than measurements from different laboratories. The global average for the seven specimen sets is also provided in Table 3 for the glass/polymer and glass/polymer/glass specimen sets. As specified in Ref. [16], one additional significant figure is provided in Table 3 to aid the assessment of the experiment.

Table 3: Summary of base results for the different makes (performed at each laboratory) of EVA, measured on the NREL-2 instrument. One additional significant figure is provided in the table as specified in [16].

	τ_{sw} {%}				τ_{rsw} {%}				*YI* {unitless}				λ_{cUV} {nm}			
CONSTRUCTION	x	s_x	s_r	s_R	x	s_x	s_r	s_R	x	s_x	s_r	s_R	x	s_x	s_r	s_R
g/p	87.873	0.187	0.293	0.293	90.562	0.068	0.289	0.289	0.602	0.049	0.088	0.088	357.95	1.11	1.27	1.27
g/p/g	88.509	0.114	0.157	0.157	91.138	0.065	0.119	0.119	0.456	0.025	0.037	0.037	357.19	0.87	1.07	1.07

Regarding the results for the different makes of EVA specimens, the g/p EVA-B, g/p EVA-E, g/p/g EVA-B, and g/p/g EVA-C specimens showed a variation about twice that of the other specimen sets (not shown). This suggests that only one laboratory (EVA-B) had a notable difference (variation) in the make of EVA specimens. As in Figure 4, the greater τ for the g/p/g specimens in Table 3 is attributed to the lesser n (and corresponding reduced reflectance loss) of the silica substrate for the g/p/g specimens. The maximum s_r and s_R values of ±0.29%, ±0.29%, ±0.09, and ±1.3nm were identified for τ_{sw}, τ_{rsw}, *YI*, and λ_{cUV}, respectively. As indicated by orange and red shading in Table 3, the maximum s_r and s_R values occur for the g/p specimens in all cases. The maximum s_r and s_R values in Table 3 will be shown in Table 4 to be ~3x greater than the practical values that may be obtained from a particular specimen using a trusted instrument, but ~1/3x the variability observed for the different materials examined and different instruments used in the R-R. This suggests that although there is an increased variability associated with the specimen make (including the silica glass and lamination process used), it does not exceed the variability associated with the choice of the encapsulation material and the instrument used for measurement.

The results of the repeatability experiment (for the same EVA specimen, both with and without replacement) are summarized in Table 4. Data in the table include τ_{sw}, the τ_{rsw}, *YI*, and λ_{cUV} (10% absolute criterion) for the seven measurement laboratories in Table 2. The average (x) and standard deviation (s_x, 2σ) are identified in Table 4 for each of the four characteristics. The global average and global standard deviation for the eight laboratories is also provided in Table 4. The s_x for the measurements taken with no replacement can be used to identify the best possible repeatability that may be obtained for the different instruments. Threshold values of ±0.03% and ±0.01 are identified for τ and *YI* measurements, respectively, from the average s_x of the same-instrument measurements. The average s_x values are indicated in orange in Table 4. The average of 0.06 nm is less than the uncertainty of ±0.5 nm, taken for λ_{cUV} based on the 1-nm resolution specified in the test procedure. The aforementioned threshold values identify the minimum increment that can be determined by the instrument for each of the four characteristics, establishing the appropriate number of significant figures.

Table 4: The average (x) and standard deviation (s_x, 2σ) for the repeatability experiment, obtained for the same glass/EVA/glass specimen measured 10x, with and without replacement. One extra significant figure is provided in the table as specified in [16].

	NO REPLACEMENT								WITH REPLACEMENT							
	τ_{sw} {%}		τ_{rsw} {%}		*YI* {unitless}		λ_{cUV} {nm}		τ_{sw} {%}		τ_{rsw} {%}		*YI* {unitless}		λ_{cUV} {nm}	
LABORATORY	x	s_x	x	s_x	x	s_x	x	s_x	x	s_x	x	s_x	x	s_x	x	s_x
Arkema	88.720	0.001	91.376	0.001	0.487	0.003	359.00	0.00	88.760	0.006	91.413	0.008	0.478	0.003	359.00	0.00
CENER	N/A	N/A	91.908	0.004	0.553	0.008	357.00	0.00	N/A	N/A	91.927	0.005	0.567	0.010	356.90	0.19
Dow Chemical	88.690	0.018	91.190	0.019	0.442	0.005	358.00	0.00	88.539	0.042	91.012	0.045	0.481	0.008	358.00	0.00
Dow-Corning	88.855	0.001	91.547	0.001	0.509	0.003	359.00	0.00	88.894	0.009	91.592	0.010	0.475	0.006	359.00	0.00
Fraunhofer	88.675	0.004	91.389	0.006	0.465	0.018	359.00	0.00	88.692	0.005	91.404	0.007	0.461	0.020	359.00	0.00
NREL-1	88.668	0.003	91.313	0.003	0.476	0.002	359.00	0.00	88.468	0.062	91.110	0.064	0.466	0.005	359.00	0.00
NREL-2	89.001	0.163	91.446	0.151	0.431	0.047	355.80	0.47	88.516	0.280	90.920	0.278	0.472	0.043	355.20	1.44
STR	88.853	0.009	91.544	0.009	0.430	0.002	359.00	0.00	88.831	0.009	91.535	0.012	0.428	0.006	358.20	0.25
x, Avg	**88.780**	**0.029**	**91.464**	**0.024**	**0.474**	**0.011**	**358.23**	**0.06**	**88.672**	**0.059**	**91.364**	**0.054**	**0.478**	**0.013**	**358.04**	**0.23**
s_x	**0.126**		**0.215**		**0.042**		**1.22**		**0.167**		**0.335**		**0.039**		**1.37**	

The measurements taken with replacement can be used to identify the best practical repeatability that may be obtained between different instruments (or laboratories). The within-laboratory measurements (performed using the same instrument) have a variability 5x (for *YI*) to 10x (for τ_{sw} and τ_{rsw}) less than the intralaboratory variability (performed using different instruments). λ_{cUV} was found to be extremely repeatable between measurements. Practical values of ±0.28%, ±0.04, and ±1.4 nm are identified for τ, *YI*, and λ_{cUV} measurements, respectively, from the maximum s_x of the measurements with specimen replacement. The variability in the λ_{cUV} measurements, however, identifies the UV-3600, custom CENER, and Lambda 1050 instruments as the most variable instruments used. The variability of the UV-3600 notably exceeded that of the other instruments. Therefore, if the UV-3600 instrument is not considered, the values of ±0.06% and ±0.02 are identified for τ and *YI* measurements, respectively, from the maximum s_x of the measurements with specimen replacement. The maximum s_x values are indicated in red in Table 4. The maximum of 0.25 nm is less than the uncertainty of ±0.5 nm, taken for λ_{cUV} based on the 1-nm resolution specified in the test procedure. These latter

values are considered the minimum increment that can be determined for a particular specimen, for each of the four characteristics.

The R-R data comparing different materials at the different laboratories was examined to aid the selection of the criterion for λ_{cUV}. Using the transmittance profiles, various criteria for λ_{cUV} were analyzed based on the corresponding s_r and s_R. The λ_{cUV} was determined for 10, 25, 50, 72, and 90% transmittance. Both absolute and relative criteria were examined, *i.e.*, x% of a chosen maximum transmission, or a transmission of x%. For the relative criteria, the transmittance at ~450 nm was used to define the maximum τ. Table 5 summarizes the relative results in addition to the Ametek and 10% absolute criteria. s_r (nominal) and s_R (nominal) are identified in Table 5 for each of the λ_{cUV} criteria. In the table, the minimal s_r and s_R is seen among the *relative* transmittance criteria at 50% for both the g/p and g/p/g specimens. Several of the criteria approach or exceed the expected ±0.5-nm resolution for λ_{cUV} (based on the 1-nm measurement increment), particularly if the variable data for material C are neglected.

Table 5: Summary of the λ_{cUV} results of the round-robin experiment. The repeatability and reproducibility are provided for several criteria used to evaluate λ_{cUV}. One extra significant figure is provided in the table as specified in [16].

		90% relative		72% relative		50% relative		25% relative		10% relative		5% relative (Ametek method)		10% absolute	
MATERIAL	CONSTRUCTION	s_r	s_R	s_r	s_R	s_r	s_R	s_r	s_R	s_r	s_R	s_r	s_R	s_r	s_R
A	g/p	0.22	0.25	0.31	0.39	0.22	0.27	0.31	0.36	0.31	0.49	0.92	0.92	0.31	0.36
B	g/p	0.38	0.38	0.31	0.33	0.31	0.38	0.58	0.63	0.49	0.59	1.13	1.16	0.58	0.63
C	g/p	2.77	3.20	2.46	2.62	0.97	1.07	0.58	0.72	0.58	0.73	2.47	2.51	0.58	0.72
D	g/p	0.87	1.04	0.62	0.64	0.65	0.65	0.76	0.76	0.87	0.92	1.19	1.21	0.76	2.28
E	g/p	0.49	0.49	0.49	0.49	0.62	0.62	0.98	0.98	2.37	2.37	1.25	1.25	0.98	0.98
***x*, Avg**	**g/p**	**0.95**	**1.07**	**0.84**	**0.89**	**0.55**	**0.60**	**0.64**	**0.69**	**0.92**	**1.02**	**1.39**	**1.41**	**0.64**	**0.99**
A	g/p/g	0.31	0.35	0.00	0.28	0.00	0.29	0.38	0.51	0.00	0.51	0.00	0.45	0.31	0.47
B	g/p/g	0.00	0.13	0.31	0.37	0.00	0.29	0.38	0.49	0.44	0.57	0.63	0.78	0.31	0.54
C	g/p/g	9.89	9.89	3.09	3.39	2.22	2.22	2.00	2.00	2.30	2.30	1.33	1.78	2.44	2.44
D	g/p/g	1.98	1.98	1.86	1.86	1.70	1.70	2.01	2.01	2.28	2.28	1.79	1.79	2.28	2.28
E	g/p/g	0.44	0.44	0.49	0.49	0.22	0.29	0.44	0.52	1.05	1.37	1.43	1.43	0.69	0.90
***x*, Avg**	**g/p/g**	**2.52**	**2.56**	**1.15**	**1.28**	**0.83**	**0.96**	**1.04**	**1.11**	**1.21**	**1.41**	**1.04**	**1.24**	**1.20**	**1.33**

The Ametek method was found to be the least repeatable and reproducible. Furthermore, it was observed during the λ_{cUV} analysis that the Ametek method (because it extrapolates results for τ = 5%) could render results that were not located on the measured data profile. Note that the presence of airborne or specimen absorbed moisture can introduce variability in optical measurements below the UV-B wavelengths.

To interpret the *relative* results in Table 5, the most repeatable and reproducible data generally correspond to that obtained at steep slopes in the transmittance profile: 20% < τ < 70%. For λ_{cUV}, one could be concerned that the initial (τ < ~10%) and final portions (τ > ~80%) of the optical transition profile have a shallow slope, and corresponding reduced repeatability and reproducibility. Furthermore, the aging and soiling of transparent polymeric materials typically results in the rounding of the final portion (τ > ~80%) of the transition profile [17],[18],[19]. The profile rounding from the aging of polymers often occurs with the formation of discoloring chromophore species [17],[18]. The profile rounding from soiling typically results from increased optical scattering as the size of the particulate contamination becomes comparable to light of shorter wavelength [19]. Both aging and soiling typically affect PV materials at wavelengths that are examined by *YI*. In contrast, the initial portion of the transition profile typically retains its slope, even with aging and soiling. The location of the initial portion of the transition profile may shift, however, if the UV absorber or UV stabilizer additives in the specimen become depleted by aging [18]. A shift in the onset of transmittance of PV materials is not typically examined in the *YI*.

The R-R participants chose to identify λ_{cUV} using the 10% absolute τ criterion. This criterion has a specific meaning (optical absorbance of 1) that is readily understood in the literature. Furthermore, the 10% definition distinguishes between the loss of UV absorber or UV stabilizer additives and the formation of chromophore species. That is, λ_{cUV} and *YI* are not redundant characteristics.

One additional pitfall in the determination of λ_{cUV} occurs for spectra with one or more UV-transmitting wavebands. For example, it is not uncommon for UV absorber additives in polymers to exhibit a doublet profile, with two absorbance peaks separated by a relatively transmitting waveband. This dilemma can be addressed by the algorithm used to determine λ_{cUV}, if the search is made to start in the visible and continued into the UV wavelengths, until the first λ_{cUV} is found.

The results of the R-R are summarized in Table 6, for τ_{sw}, τ_{rsw}, *YI*, and λ_{cUV}. The average (x), standard deviation (s_x, 1σ), repeatability (s_r, nominal), and reproducibility (s_R, nominal) are identified in Table 6 for the four characteristics examined in the standard. For the R-R analysis, s_r now emphasizes repeatability within the same laboratory, whereas s_R emphasizes reproducibility between different laboratories. As identified in orange, the maximum s_r values of ±0.78%, ±0.63%, ±0.27, and ±2.4 nm are identified for τ_{sw}, τ_{rsw}, *YI*, and λ_{cUV}, respectively. The maximum s_R values of ±0.88%, ±0.90%, ±0.46, and ±2.4 nm are similarly identified in red for τ_{sw}, τ_{rsw}, *YI*, and λ_{cUV}. For τ and *YI*, the s_r and s_R of the hazy polymer, material D, approaches 10x that of the other materials. This identifies that haze can increase s_r and s_R. Material C, which had a λ_{cUV} < 250 nm, also had the greatest s_r and s_R values for λ_{cUV}. The s_r was generally less than the s_R, *i.e.*, the between laboratory variation is larger than the internal laboratory variation. As in Table 3 and Table 4, the τ_{sw} in Table 6 is typically less than the τ_{rsw}. As in Figure 4, the τ for the g/p specimens is typically less than that of the g/p/g specimens, which most likely results from refractive index difference between the polymers and the glass.

Table 6: Summary of the round-robin experiment results. One extra significant figure is provided in the table as specified in [16].

		τ_{sw} {%}				τ_{rsw} {%}				*YI* {unitless}				λ_{cUV} {nm}			
MATERIAL	CONSTRUCTION	x	s_x	s_r	s_R	x	s_x	s_r	s_R	x	s_x	s_r	s_R	x	s_x	s_r	s_R
A	g/p	89.178	0.088	0.145	0.161	91.148	0.078	0.117	0.134	0.528	0.020	0.029	0.034	356.58	0.31	0.31	0.36
B	g/p	87.505	0.056	0.167	0.167	90.098	0.055	0.081	0.093	0.765	0.032	0.034	0.046	381.33	0.41	0.58	0.63
C	g/p	92.573	0.143	0.227	0.254	93.701	0.141	0.241	0.266	0.325	0.062	0.029	0.067	206.76	0.45	0.58	0.72
D	g/p	84.525	0.818	0.257	0.852	85.743	0.858	0.217	0.882	2.422	0.370	0.128	0.388	356.13	0.37	0.76	2.28
E	g/p	86.834	0.043	0.264	0.264	89.186	0.058	0.155	0.156	2.895	0.082	0.234	0.234	365.63	0.63	0.98	0.98
x	g/p	88.12	N/A	0.21	0.34	89.98	N/A	0.16	0.31	1.39	N/A	0.09	0.15	333.3	N/A	0.6	1.0
A	g/p/g	89.509	0.111	0.058	0.123	91.627	0.102	0.063	0.118	0.490	0.019	0.024	0.030	357.42	0.37	0.31	0.47
B	g/p/g	88.158	0.073	0.080	0.104	90.668	0.072	0.050	0.086	0.704	0.023	0.026	0.033	381.13	0.46	0.31	0.54
C	g/p/g	91.215	0.101	0.777	0.777	93.089	0.084	0.149	0.162	0.468	0.091	0.177	0.178	210.19	0.41	2.44	2.44
D	g/p/g	84.700	0.641	0.643	0.875	85.844	0.680	0.626	0.897	2.732	0.378	0.272	0.456	360.54	0.28	2.28	2.28
E	g/p/g	87.762	0.152	0.595	0.595	89.893	0.072	0.104	0.121	2.556	0.068	0.075	0.097	360.63	0.62	0.69	0.90
x	g/p/g	88.27	N/A	0.43	0.49	90.22	N/A	0.20	0.28	1.39	N/A	0.11	0.16	334.0	N/A	1.2	1.3

The range of optical transmittance for the materials in Table 6 is at least 5%, several times greater than the s_r or s_R. The different performance intrinsic to the materials examined in the R-R is readily observed if the transmittance profiles are superimposed. Because the thickness of the polymer layer is nominally the same (z= 0.5 mm), the different performance is attributed to the base materials and the formulations. A manufacturer may also wish to consider characteristics in addition to τ, including: electrical resistivity; elastic modulus; moisture permeability; and UV-durability, when selecting an encapsulation for use in PV modules. The maximum s_r and s_R values in Table 6 are taken as the conservative estimate for error in τ_{sw}, τ_{rsw}, *YI*, and λ_{cUV}. To explain, if the 1σ average in Table 6 were used to evaluate the 95% limits, the maximum s_r and s_R values slightly exceed the confidence limits identified in Ref. [16], where $r = 2.8 \cdot s_r$ and $R = 2.8 \cdot s_R$. The τ profiles varied the most between the laboratories for the hazy material D. The λ_{cUV} of material C approaches the limitations of measurement for PMT detectors in a moisture-containing atmosphere, corresponding to the greatest s_r and s_R values for λ_{cUV}. As in Figure 3, Figure 4, and Figure 5, and further examined in Ref. [13], all of the encapsulation materials have absorbing bands in the IR wavelengths; therefore, it is not surprising that the τ_{sw} is less than the τ_{rsw} (which only extends to 1250 nm). Lastly, the lesser τ for the g/p specimens is consistent with Figure 4, where the

difference was attributed to the lesser n (better matched to air) of silica. In contrast, because the n of material C is uniquely less than that of silica, a greater reflectance loss is expected for the g/p/g specimens, as observed in Table 6.

4. CONCLUSIONS

A round-robin experiment (R-R) was conducted to support a recently proposed standardized test method for the measurement of PV encapsulation materials. Key results include: (1) Threshold values of ±0.03%, ±0.01, and ±0.5 nm were identified for transmittance (τ), yellowness index (YI), and UV cut-off wavelength (λ_{cUV}) measurements as the minimum increment that can be determined by contemporary spectrophotometer instruments for each of the characteristics. Practical values of ±0.06%, ±0.02, and ±0.5 nm are identified for τ, YI, and λ_{cUV} as the minimum increment that can be determined for a particular specimen using a trusted instrument, for each of the characteristics. (2) The criterion 10% of the absolute transmittance was shown to provide a reasonable repeatability (s_r) and reproducibility (s_R), with respect to other relative or extrapolated criteria. The 10% criterion for λ_{cUV} also helps to distinguish between the loss of UV additives (absorbers and stabilizers) and the formation of chromophore species. (3) The maximum s_r values of ±0.78%, ±0.63%, ±0.27, and ±2.4 nm were identified for τ_{sw}, τ_{rsw}, YI, and λ_{cUV}, respectively in the R-R. The maximum s_R values of ±0.88%, ±0.90%, ±0.46, and ±2.4 nm were identified for τ_{sw}, τ_{rsw}, YI, and λ_{cUV}. (4) The maximum s_r and s_R values of ±0.29%, ±0.29%, ±0.09, and ±1.3 nm were identified for τ_{sw}, τ_{rsw}, YI, and λ_{cUV}, respectively, for specimens of the same material made at the different laboratories. This suggests that although there is an increased variability associated with the specimen make (including the silica glass and lamination process), it does not exceed the variability associated with the choice of encapsulation material and/or instrument used for measurement.

Additional experiments demonstrated the benefit of using a depolarizer, the representative performance for silica substrates and superstrates, and a baselining protocol to correct port effects in single-beam spectrophotometer instruments. Although haze-prone materials were found to limit τ and YI, it is uncertain whether material discoloration would similarly limit transmittance measurements.

ACKNOWLEDGMENTS

The authors are grateful to Mikel Ezquer Mayo of Fundación CENER-CIEMAT, Johannes Hanek of Fraunhofer ISE, and Scott Deibert and Dr. Mike Kempe of the National Renewable Energy Laboratory for their help with measurements and discussion of the results. This work was supported by the U.S. Department of Energy under Contract No. DE-AC36-08GO28308 with the National Renewable Energy Laboratory. Instruments and materials are identified in this paper to describe the experiments. In no case does such identification imply recommendation or endorsement by NREL.

REFERENCES

[1] Jordan, D.C., Wohlgemuth, J.H., and Kurtz, S.R., "Technology and Climate Trends in PV Module Degradation," *Proc. Euro PVSEC*, 118–124 (2012).

[2] "ISO 13468-2 Plastics—Determination of the Total Luminous Transmittance of Transparent Materials—Part 2: Double-beam instrument," International Electrotechnical Commission: Geneva, 1–6 (1999).

[3] "ASTM E903-12 Standard Test Method for Solar Absorptance, Reflectance, and Transmittance of Materials Using Integrating Spheres," ASTM International, West Conshohocken, PA, 1–17 (2012).

[4] "ASTM E1175–87 Method for Determining Solar or Photopic Reflectance, Transmittance, and Absorptance of Materials Using a Large Diameter Integrating Sphere," ASTM International, West Conshohocken, PA, 1–4 (2009).

[5] "ASTM E424-71 Standard Test Methods for Solar Energy Transmittance and Reflectance (Terrestrial) of Sheet Materials," ASTM International, West Conshohocken, PA, 1–6 (2007).

[6] "IEC 60904-3 Photovoltaic devices. Part 3: Measurement Principles for Terrestrial Photovoltaic (PV) Solar Devices with Reference Spectral Irradiance Data," International Electrotechnical Commission: Geneva, (submitted).

[7] Beckman, W.A., Bugler, J.W., Cooper, P.I., Duffie, J.A., Dunkle, R.V., Glaser, P.E., Horigome, T., Howe, E.D., Lawand, T.A., Van der Mersch, P.L., Page, J.K., Sheridan, N.R., Szokolay, S.V., and Ward, G.T., "Units and Symbols in Solar Energy", *Solar Energy*, **21**, 1978, 65-68.

[8] Green, M.A., Emery, K., Hishikawa, Y., Warta, W., and Dunlop, E.D., "Solar Cell Efficiency Tables (version 41)," *PIP: Res. App*. **21**, 1–11 (2013).

[9] "ISO 11664-2 Colorimetry-Part 2: CIE Standard Illuminants," International Electrotechnical Commission: Geneva, 1–14 (2007).

[10] "ISO 11664-1 Colorimetry-Part 1: CIE Standard Colorimetric Observers," International Electrotechnical Commission: Geneva, 1–29 (2007).

[11] "ASTM E308-06 Standard Practice for Computing the Colors of Objects by Using the CIE System," ASTM International, West Conshohocken, PA, 1–34 (2006).

[12] "ASTM E313-05 Standard Practice for Calculating Yellowness and Whiteness Indices from Instrumentally Measured Color Coordinates," ASTM International, West Conshohocken, PA, 1–6 (2005).

[13] Miller, D.C., Kempe, M.D., Kennedy, C.E., and Kurtz, S.R., "Analysis of Transmitted Optical Spectrum Enabling Accelerated Testing of Multi-Junction CPV Designs," *Opt. Eng*. **50** (1), 013003 (2011).
[14] McIntosh, K.R., Powell, N.E., Norris, A.W., Cotsell, J.N., and Ketola, B.M., "The Effect of Damp-Heat and UV Aging Tests on the Optical Properties of Silicone and EVA Encapsulants," *PIP: Res. App*. **19** (3), 294–300 (2010).
[15] "ASTM D7778-12 Standard Guide for Conducting an Interlaboratory Study to Determine the Precision of a Test Method," ASTM International, West Conshohocken, PA, 1–10 (2012).
[16] "ASTM E691-12 Standard Practice for Conducting an Interlaboratory Study to Determine the Precision of a Test Method," ASTM International, West Conshohocken, PA, 1–22 (2012).
[17] Pern, FJ., "Factors That Affect the EVA Encapsulant Discoloration Rate Upon Accelerated Exposure," *Solar Energy Solar Mater.* **41/42,** 587–615 (1996).
[18] Shioda, T., "UV Accelerated Test Based on Analysis of Field Exposed PV Modules," Proc SPIE 2011, 8112–17.
[19] Miller, D.C., Kurtz, S.R., "Durability of Fresnel Lenses: A Review Specific to the Concentrating Photovoltaic Application," *Solar Energy Materials and Solar Cells* **95** (8), 2037–2068 (2011).